Available online at www.sciencedirect.com
SCIENCE DIRECT®
Physics of the Earth and Planetary Interiors 154 (2006) 196–207
PHYSICS OF THE EARTH AND PLANETARY INTERIORS
www.elsevier.com/locate/pepi

Lower mantle dynamics with the post-perovskite phase change, radiative thermal conductivity, temperature- and depth-dependent viscosity

Ctirad Matyska[a,*], David A. Yuen[b]

[a] *Department of Geophysics, Faculty of Mathematics and Physics, Charles University, V Holešovičkách 2, 180 00 Praha 8, Czech Republic*
[b] *Department of Geology and Geophysics and Minnesota Supercomputing Institute, University of Minnesota, Minneapolis, MN 55455-0219, USA*

Received 3 April 2005; accepted 9 October 2005

Abstract

The new post-perovskite phase near the core–mantle boundary has important ramifications on lower mantle dynamics. We have investigated the dynamical impact arising from the interaction of temperature- and depth-dependent viscosity with radiative thermal conductivity, up to a lateral viscosity contrast of 10^4, on both the ascending and descending flows in the presence of both the endothermic phase change at 670 km depth and an exothermic post-perovskite transition at 2650 km depth. The phase boundaries are approximated as localized zones. We have employed a two-dimensional Cartesian model, using a box with an aspect-ratio of 10, within the framework of the extended Boussinesq approximation. Our results for temperature- and depth-dependent viscosity corroborate the previous results for depth-dependent viscosity in that a sufficiently strong radiative thermal conductivity plays an important role for sustaining superplumes in the lower mantle, once the post-perovskite phase change is brought into play. This aspect is especially emphasized, when the radiative thermal conductivity is restricted only to the post-perovskite phase. These results revealed a greater degree of asymmetry is produced in the vertical flow structures of the mantle by the phase transitions. Mass and heat transfer between the upper and lower mantle will deviate substantially from the traditional whole-mantle convection model. Streamlines revealed that an overall complete communication between the top and lower mantle is difficult to be achieved.

Keywords: Post-perovskite phase transition; Radiative thermal conductivity; Temperature- and pressure-dependent viscosity; Asymmetric mantle convection

1. Introduction

The boundary between the lowermost mantle and outer core, is the most active, but least understood region of the Earth's deep interior. Heat- transfer across the core–mantle boundary (CMB) appears fundamental in promoting large-scale instabilities including plume clusters and superplume upwellings in the lower mantle (Maruyama, 1994; Zhao, 2001, 2004; Takeuchi and Kobayashi, 2004; Schubert et al., 2004), which impact not just on the lower mantle but also the entire mantle. Seismically, the lowermost 200–300 km of Earth's mantle is anomalous. Geophysical investigations over the last decade show that D″, the approximate 100–350 km thick seismic layer located near the CMB and characterized generally by a strong negative shear velocity and small compressional velocity gradients,

* Corresponding author. Tel.: +420 2 21912538; fax: +420 2 21912555.
E-mail address: Ctirad.Matyska@mff.cuni.cz (C. Matyska)

0031-9201/$ – see front matter © 2005 Elsevier B.V. All rights reserved.
doi:10.1016/j.pepi.2005.10.001

is both seismically heterogeneous and anisotropic on vertical and horizontal length-scales down to about tens of kilometers (e.g. Garnero, 2000; Lay et al., 2004).

The discovery in 2004 of the new perovskite (pv) to post-perovskite (ppv) phase transition in the deep mantle near the D″ layer (Murakami et al., 2004; Tsuchiya et al., 2004; Oganov and Ono, 2004; Iitaka et al., 2004), from X-ray diffraction studies and first principles quantum-mechanical calculations, has recently added exciting and potentially far-reaching consequences. Already, it is clear that this new phase transition can profoundly influence the dynamics of the D″ layer, and by implication the CMB (Nakagawa and Tackley, 2004; Matyska and Yuen, 2005). Matyska and Yuen (2005) have also found that the presence of this new phase transition could make the D″ layer highly unstable and inhibits the generation of thick deep mantle plumes. They found that radiative thermal conductivity is needed for maintaining large-scale upwellings (Matyska et al., 1994) in the lower mantle. In this connection, the influence of the phonon contribution to the thermal conductivity is likely to be almost negligible in the lower mantle because of increasing temperature above the Debye temperature (Hofmeister and Yuen, submitted for publication).

Thus, the major difference between the dynamical works of Nakagawa and Tackley (2004) and Matyska and Yuen (2005) on the post-perovskite phase is the usage of radiative thermal conductivity in the model. Nakagawa and Tackley (2004) employed a depth-dependent thermal conductivity model, while Matyska and Yuen (2005) picked a strongly radiative thermal conductivity, which is motivated by the works of Hofmeister (1999, 2005) and reinforced by the laboratory inference by Badro et al. (2004) on the basis of the high spin to low spin electronic transition of Fe^{2+} in deep mantle silicates and oxides, see also (Li et al., 2005). The rheology employed by Nakagawa and Tackley is also different from that used by Matyska and Yuen (2005). In Nakagawa and Tackley (2004) there is no local viscosity maximum peaking by a factor of around 50–100 in the mid-lower mantle, as proposed by Forte and Mitrovica (2001) and Mitrovica and Forte (2004) on the basis of post-glacial rebound and dynamic geoid modelling, while in the depth-dependent viscosity model of Matyska and Yuen (2005) this particular feature in the lower mantle viscosity profile is retained. The viscosity variations in the lower mantle caused by changes of temperature are not as strong as in the upper mantle but they are nonetheless important in lower mantle dynamics, especially in D″ layer (e.g. Yuen and Peltier, 1980; Olson et al., 1987). This is the reason why temperature-dependent viscosity has been included into our rheological model.

The presence of this post-perovskite phase change at the base of the mantle has the potential of producing other unexpected symmetry-breaking features (e.g. Schuster, 1984) in mantle dynamics, such as the difference in the fates between the descending slabs and the hot upwellings, especially with the presence of two physically competing mechanisms of variable viscosity and radiative thermal conductivity. In this study, we will monitor the differences in the behavior between the upwelling and downwellings for different amounts of lateral viscosity contrasts due to temperature and strengths in the radiative thermal conductivity. Hauck et al. (1999) and Dubuffet et al. (2000) have already found that subducting slabs undergo thermal assimilation much more readily with the presence of variable thermal conductivity. This process would also be enhanced by negative buoyancy caused by an upward undulation of the post-perovskite phase interface and probably also by weakening of the bottom portion of the descending slab due to the latent heat released from this phase transition and the attendant rheological softening. In Section 2, we discuss about our numerical and physical models of variable viscosity and radiative thermal conductivity. The results comparing the interplay between rheology and radiative conductivity are given in Section 3, where, in contrast to past studies, we have also studied the interesting situation of an enhanced thermal radiative conductivity layer only for the post-perovskite phase.

2. Model description

We have employed here the streamfunction formulation of 2-D thermal convection model within the extended Boussinesq approximation (e.g. Christensen and Yuen, 1985), in which the surface dissipation number $Di = \alpha_s g D/c_p$ (α_s is the surface thermal expansivity, g the gravity acceleration, D the thickness of the mantle and c_p is the specific heat under a constant pressure) is set to 0.5. Standard values of the material properties of the mantle have been used (e.g. Turcotte and Schubert, 2002). The mathematical description of this finite-difference numerical model has already been published previously by Matyska and Yuen (2000, 2001, 2002).

One strong endothermic change depicting the spinel to perovskite phase transition (spv), with the buoyancy parameter P appearing linearly in the momentum equation $P = (\Delta\rho/\alpha_s\rho^2 g D)(\mathrm{d}p/\mathrm{d}T)$ equal to -0.15 has been included at the dimensionless depth $z = 0.23$ (this corresponds to 670 km depth) where $z \in \langle 0, 1\rangle$ is normalized by the depth D at the CMB (ρ is a reference av-

erage density taken for the entire mantle, $\Delta\rho$ the density jump due to the phase change under consideration and $\mathrm{d}p/\mathrm{d}T$ is its Clapeyron slope). The second phase change has been considered at the depth $z = 0.92$, which corresponds to a depth of 2650 km (see, e.g. Tsuchiya et al., 2004). We consider an exothermic phase change with a density change in the range of a couple of percent and Clapeyron slopes between 8 and 10 MPa/K (Tsuchiya et al., 2004). We note that the parameter range of P associated with the post-perovskite (ppv) transition is different from the spinel to perovskite (spv) transition in that $|P|$ for spv is larger than in the case of ppv transition because of much larger density change, although $|\mathrm{d}p/\mathrm{d}T|$ is lower.

The variation in the dimensionless depth-dependent thermal expansivity profile has been parameterized to

$$\alpha(z) = \frac{8}{(2+z)^3}, \tag{1}$$

see, e.g. Zhao and Yuen (1987). Thus, the thermal expansivity decreases by 8/27 across the mantle.

Instead of using just the depth-dependence for describing the viscosity profile with a local maximum in the mid-lower mantle (e.g. Ricard and Wuming, 1991; Forte and Mitrovica, 2001; Mitrovica and Forte, 2004), we have included a temperature-dependent portion $f(T)$ as well in a multiplicative manner in viscosity $\eta(z, T) = \eta_0(z)f(T)$, where $\eta_0(z)$ is the particular viscosity profile with a local maximum at around 1800 km in depth used by Hanyk et al. (1995) for post-glacial rebound modelling and by Matyska and Yuen (2005) in mantle convection models with the post-perovskite transition. We have elected to use $\eta_0(z)$ because the peak of the viscosity profile in the mid-lower mantle may be related to some other physical transitions, such as electronic (Badro et al., 2003; Li et al., 2005). T is the dimensionless temperature, $T = 0$ at the surface and $T = 1$ at the core–mantle boundary. As the dimensional temperature T' is related to T by means of the temperature increase ΔT across the mantle: $T' = \Delta T(T_0 + T)$, the dimensionless surface temperature $T_0 = 0.08$ corresponds to around 300 K for a temperature increase ΔT of 3600 K (van den Berg and Yuen, 1998). The temperature-dependent part $f(T)$ is given by the Arrhenius form of a thermally activated process, being proportional to $\exp(A/T)$, where A is related to the activation energy of Newtonian mantle creep:

$$f(T) = \exp\left(10.0\left(\frac{0.6}{0.2+T} - 1\right)\right), \tag{2}$$

e.g. Davies (1999). Taken together, we can write down this particular composite temperature- and depth-dependent viscosity relationship as

$$\eta(z, T) = [1 + 214.3z\exp(-16.7\,(0.7 - z)^2)] \times \min\{F_T, \max\{F_T^{-1}, f(T)\}\}, \tag{3}$$

where the functional dependence of z gives rise to the lower mantle viscosity maximum. As to the prefactor F_T determining sensitivity of viscosity to temperature differences, we have chosen either $F_T = 10$ or 100 in most of the models. As the lateral lower mantle viscosity contrasts are estimated to be of $O(10^3)$ from the activation energy of perovskite around O(200 kJ/mol) (Marton and Cohen, 2002) and high background lower mantle temperature of 3000– 4000 K, our choices of F_T seem to be able to produce sufficient lateral viscosity contrasts.

We have considered both constant dimensionless thermal conductivity $k = 1$ and variable dimensionless thermal conductivity in the form

$$k = 1 + g(z)(T_0 + T)^3. \tag{4}$$

We have here neglected the temperature-dependence of the phonon contribution to the thermal conductivity, because above the Debye temperature the lattice contribution to the thermal conductivity becomes a constant (Hofmeister and Yuen, submitted for publication). The second term describes the radiative transfer of heat. The surface thermal conductivity k_s is taken to be that from olivine (e.g. Brown, 1986). The factor $g(z)$ in Eq. (4) is a measure of the importance of radiative heat transport. We have employed the value $g(z) = 10.0$, which was already used in the studies by Matyska et al. (1994) and Matyska and Yuen (2005), as well as a weaker radiative term with $g(z) = 5.0$. In the final model for the thermal conductivity we have considered $g(z) = 10.0$ only within the bottom 240 km associated with the D″ layer, i.e. $g(z)$ expressing the magnitude of radiative thermal conductivity was set equal to zero above the post-perovskite phase change boundary. This last model was motivated by the fact that this phase change may be accompanied by a change of opacity due to electronic rearrangements (e.g. Badro et al., 2004; Li et al., 2005). In such a model, we thus assume that the radiative heat transfer is non-negligible only in the D″ layer and hence may be omitted in the mantle above.

We have fixed both the surface Rayleigh number, $Ra_\mathrm{s} \equiv \rho_\mathrm{s}^2 c_\mathrm{p} \alpha_\mathrm{s}\, \Delta T g D^3/\eta_\mathrm{s} k_\mathrm{s} = 10^7$ (η_s is the surface viscosity and k_s is the surface thermal conductivity) and the dimensionless internal heating $R \equiv QD^2/k_\mathrm{s}\,\Delta T = 3$, where Q denotes volumetric the heat sources throughout the mantle. This value corresponds approximately to one-fourth of the whole-mantle chondritic heating (e.g. Leitch and Yuen, 1989). Our internal heating employed

is relatively modest because too much internal heating, such as chondritic abundance of radioactivity in the presence of radiative thermal conductivity would increase the temperature in the lower mantle too much as to cause wholesale melting (van den Berg et al., 2002).

Note that the depth-dependence of thermal expansivity, the temperature-dependence of thermal conductivity together with the depth- and temperature-dependence of viscosity result approximately in the effective Rayleigh number of more than one order of magnitude lower, $O(10^6)$ close to the CMB, which is an important factor for maintaining the stability of the lower mantle plumes (e.g. Hansen et al., 1993).

The final set of equations consists of the momentum equation, which becomes a fourth-order linear elliptic equation for the streamfunction $\psi(x, z, t)$ with both laterally and vertically varying coefficients because of the presence of $\eta(z, T)$, where the dependence on time t arises from a time-dependence of the inhomogeneous forcing term of this equation, which is due to both thermal buoyancy and the two localized phase transitions. This elliptic equation is solved by a conjugate gradient iterative scheme. The governing equation for T represents a time-evolutionary advection–diffusion equation, which is solved by a second-order Runge–Kutta scheme in time and a second-order central finite-difference scheme in space. Most of the computations have been carried out in a wide box with an aspect-ratio of 10 to avoid the influence of side-boundaries, where the reflecting boundary conditions were used. One calculation has been carried out in an aspect-ratio six box, as done previously (Matyska and Yuen, 2005). We have used 1281×129 equally distributed nodal points for the computations in the box with the aspect-ratio of 10 and a correspondingly reduced grid in the horizontal direction for the model with the aspect-ratio reduced to 6. All of our integrations have been carried out to at least 0.01 dimensionless time, corresponding to about the age of the Earth. The results are thus represented in "statistical equilibrium", i.e. for the cases where the influence of the initial conditions to integral quantities like averaged temperature or heat flow are negligible. In the terminology of non-linear dynamics, we display the states, which are close to the strange attractors of the studied non-linear systems (see, e.g. Schuster, 1984).

3. Results

Matyska and Yuen (2005) previously focussed on the influence of the ppv transition on the style of mantle convection with only a depth-dependent viscosity (i.e. with $F_T = 1$). We have studied a range of buoyancy parameters P in a box with an aspect-ratio of six. In Fig. 1 we remind the reader of our previous results obtained for endothermic spinel to perovskite transition with $P = -0.15$ and ppv transition with $P = 0.1$, which corresponds to a strong exothermic phase change with a significant positive Clapeyron slope $\mathrm{d}p/\mathrm{d}T$ of around 10 MPa/K and density change of a couple of percent. We can clearly see that the role played by the thermal conductivity k can be crucial, as convection with constant k is characterized by a development of many lower boundary layer instabilities, which are attracted to an already existing plume. We have found that such an event is repeated many times during the temporal evolution. The temperature contrast between the interior of plumes and the ambient mantle is about 0.5 in the dimensionless unit which is rather high. On the other hand, with radiative thermal conductivity we can discern the stabilization of mantle convection and the emergence of

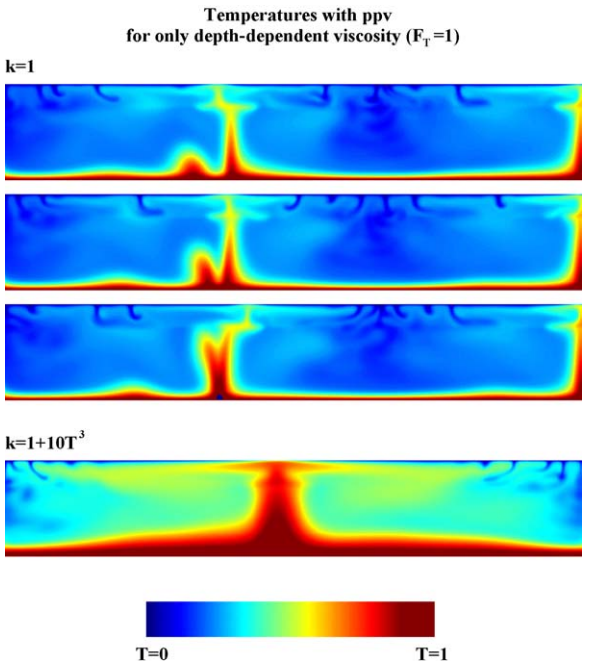

Fig. 1. Typical snapshots of the temperature field for a long time scale. An endothermic phase change with $P = -0.15$ at the depth of 670 km and an exothermic phase change with $P = 0.10$ at the depth of 2650 km were included. Viscosity is only depth-dependent, i.e. $F_T = 1$, see also paper by Hanyk et al. (1995) and Mitrovica and Forte (2004). Panels obtained for constant thermal conductivity $k = 1$ show the plume–plume interactions, whereas thermal conductivity with strong radiative term ($k = 1 + 10(T_0 + T)^3$) results in a stable lower mantle superplume. Dimensionless time-steps between the subsequent upper panels are 8×10^{-4}. The red color represents the maximum temperature, while the dark blue color denotes the minimum temperature. The medium temperature is given by the cold to warm transition from the green to yellow color. (For interpretation of the references to color in this figure legend, the reader is referred to the web version of this article.)

a more-or-less stationary large upwelling in the lower mantle. Moreover, an increase of ambient mantle temperature resulted in lower temperature contrast between the mantle and the plume, which seems to be more plausible (Dubuffet et al., 2002) and which is also important for the dynamics of the D″ topography as discussed by Matyska and Yuen (2005). The question then arises as to whether these conclusions still remain valid in the case of a more realistic temperature-dependent viscosity. To avoid potential influence of the side-boundaries, we have also increased the aspect-ratio of the convection box to 10. With a larger aspect-ratio box we can also monitor better the dynamics of the cold downwellings. Since the thermodynamic parameters of ppv transition became recently more fixed we need not consider the buoyancy parameter to be a free parameter as in our previous study but we have chosen only the magnitude of $P = 0.1$ here to incorporate this phase change into the models.

First, we concentrated on the role played by the radiative heat- transfer in the absence of the ppv phase change and demonstrated that the pattern of convection again differs substantially, if we compare the temperature fields obtained for constant thermal conductivity $k = 1$ with those for $k = k(T)$, where the radiative thermal conductivity is added. The results are summarized in Fig. 2, see also Dubuffet et al. (2002) and van den Berg et al. (2002) for the influence of radiative thermal conductivity. This effect is displayed here for a temperature-dependence of viscosity with $F_T = 10$, which can thus produce two orders of magnitude lateral change of viscosity. No ppv transition is considered, i.e. the only phase transition is that at the depth of 670 km with endothermic buoyancy parameter $P = -0.15$. Purely constant thermal conductivity, i.e. $k = 1$, results in lower average temperatures with unstable downwellings as well as smaller unstable plumes, whereas in the case of strong radiative conductivity superplumes are produced. Their locations remain relatively stable but their internal dynamics is governed by generation of lower boundary layer instabilities, which are being constantly attracted to the superplumes (e.g. Vincent and Yuen, 1988).

The role played by the ppv transition in convection dynamics is also interesting (see Fig. 3). In the case of constant thermal conductivity, $k = 1$, the presence of ppv transition, modelled here by means of the exothermic buoyancy parameter $P = 0.1$, enhances the generation of smaller unstable plumes, while the case with radiative thermal conductivity, $k = k(T)$, is characterized by minor changes. There is a latent heat absorbed by superplumes from this positive Clapeyron slope phase change but we have not found a remarkable change in superplume dynamics. Therefore, the patterns of mantle convection in which large upwellings are developed (e.g. Su and Dziewonski, 1991; Zhao, 2001, 2004) can be obtained by an increase of thermal conductivity in the lower mantle. The time-dependence of convection in the $k = 1$ case can clearly be visualized by the streamlines. On the other hand, variable thermal conductivity produces higher convective velocity, since an increase of temperature due to the increase of thermal conductivity yields a lower average viscosity with an abrupt increase just at the cold downwelling and a greater buoyancy of large upwellings, but the convection pattern in the lower mantle remains stable. We emphasize here that the contour interval of non-dimensional streamlines is 100 and is the same for all panels in the figures of this paper. The dimensionless velocity is defined by the relation $\mathbf{v} = (\partial\psi/\partial z, -\partial\psi/\partial x)$, where ψ is the streamfunction. The maximal dimensionless velocity achieved in the bottom panel of the figure is thus about 5000. As the velocity is scaled by the factor $k_s/\rho c_p D$, which is of the order O(10^{-3} cm/year), such an velocity represents the dimensional value of about 5 cm/year.

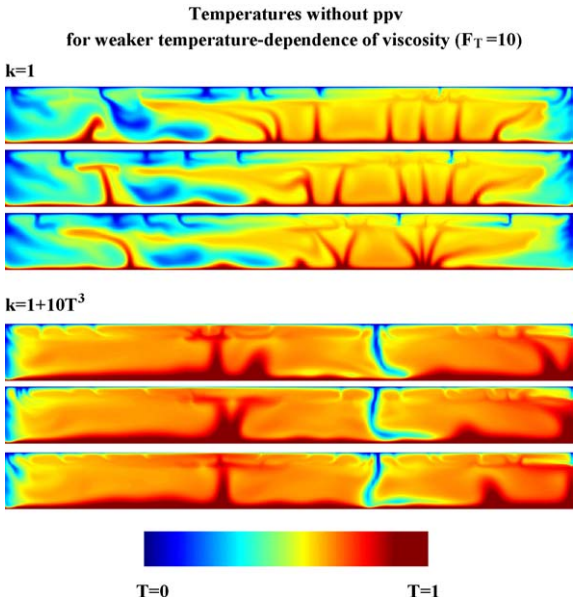

Fig. 2. Typical snapshots of the temperature field in the calculations, where an endothermic phase change with $P = -0.15$ at the depth of 670 km and no phase change at the depth of 2650 km were included. Viscosity is also weakly temperature-dependent ($F_T = 10$). Results for both constant thermal conductivity $k = 1$ (with dimensionless time-steps equal to 10^{-3}) and variable thermal conductivity $k = 1 + 10(T_0 + T)^3$ (with dimensionless time-steps equal to 4×10^{-4}) are displayed.

In this study, we aim to focus our attention also on the behavior of cold downwellings in the presence of ppv transition. In order to capture better the differences between the cold and hot areas, we have increased the

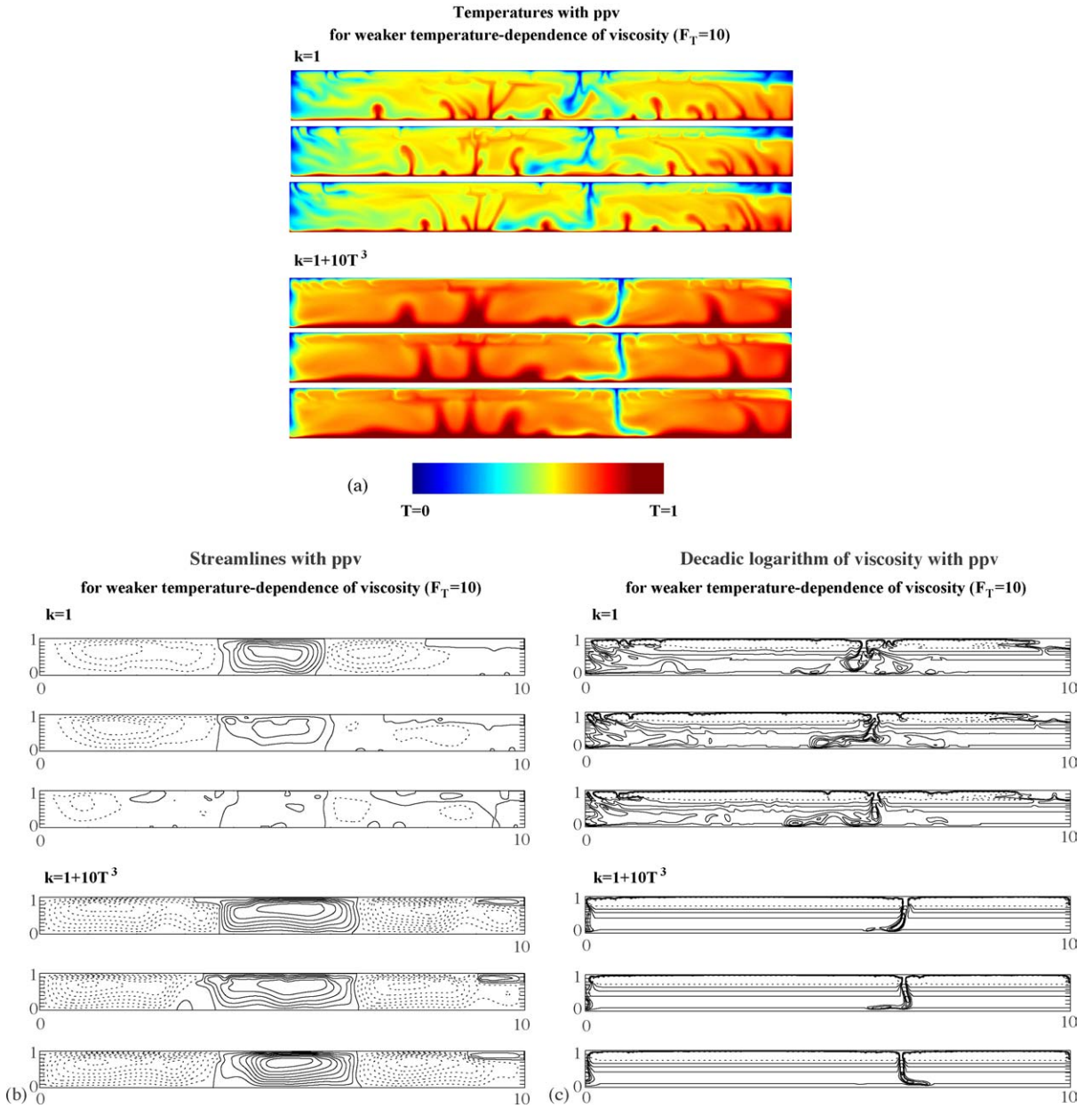

Fig. 3. (a) The same as in Fig. 2 but an exothermic phase transition with $P = 0.10$ was added at 2650 km depth. (b) Streamlines of the mantle flow corresponding to the temperature fields at each time-step shown in (a). The streamfunction is equal to zero on all sides of the box and the contour interval of streamlines is 100 in dimensionless units. The contour interval is kept the same in all panels. The solid lines display the zero and negative values and the dashed lines show the positive values of the streamfunction. (c) Decadic logarithm of dimensionless viscosity. Dashed lines show negative values and solid lines mark zero and positive values. The contour interval is 0.5 in all panels.

temperature sensitivity of viscosity by the choice $F_T = 100$, i.e. maximal admissible lateral changes of viscosity are some four orders in magnitude. As the temperature-dependence of radiative thermal conductivity of k seems to be crucial, we will now consider only the cases with $k = k(T)$.

If there is no ppv transition, from time to time we can obtain a cold downwelling, which extends from the surface down to the core–mantle boundary. Such a situation is followed by detachment of a cold blob lying then at the core–mantle boundary as displayed in Fig. 4. At first glance, the convection dynamics in the presence of ppv

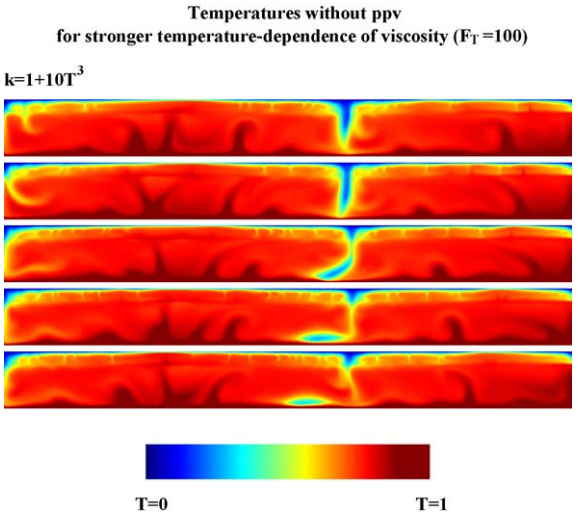

Fig. 4. The same as in Fig. 2 but stronger temperature-dependence of viscosity ($F_T = 100$) was considered and only the case $k = 1 + 10(T_0 + T)^3$ is shown. Dimensionless time-steps between the subsequent panels are 8×10^{-4}.

transition (see Fig. 5), seems to be very similar to the previous case but the detachment of a cold blob occurs a little earlier during the creation of subducting cold slab. Seismic tomography studies showed that stagnant cold slabs are only directly visible in the shallow part of the lower mantle (e.g. van der Hilst et al., 1991; Fukao et al., 1992; Zhao, 2004). Possible explanation of this phenomenon is that the exothermic post-perovskite phase change liberates some amount of heat and, moreover, is able to slightly speed up downflow by additional negative buoyancy caused by a shift of phase change topography to lower depths, which serves to cause slab-detachment in the deeper lower mantle. We note that the heat liberated is proportional to the product $T(\mathrm{d}p/\mathrm{d}T)$; both factors are high for the ppv transition. Signs of layered convection can be discernible in the streamline patterns, which clearly show maximum horizontal velocities just below the 670 km interface. Moreover, a weaker small-scale convection in the upper mantle is also present. Thus, there exists a dynamical connection between this deep mantle phase transition and upper mantle circulation in our model.

Note that an increase of temperature sensitivity of viscosity resulted in its decrease outside cold downwellings as it is clear from comparison of Figs. 3c and 5c. Nevertheless, the main characteristics of the lower mantle dynamics – an interplay between large more or less stable hot upwellings and local cold downwellings – remain similar in both cases due to the presence of a strong radiative heat transfer. In order to demonstrate further the importance of temperature-dependence of thermal conductivity in maintaining megaplumes, we have also included temporal developments of the temperature field for a stronger temperature-dependence in the viscosity (up to 10^4) in the presence of the ppv transition but with a reduced radiative thermal conductivity, which is one-half of our usual value (e.g. Matyska and Yuen, 2005), i.e.

$$k = 1 + 5(T_0 + T)^3. \tag{5}$$

The radiative thermal conductivity is weaker by 50% and the consequence of such a change is that the megaplume structure is able to change its morphology to a cluster consisting of smaller plumes (e.g. Schubert et al., 2004) and does not appear as a single coherent entity (see Fig. 6). On the other hand, the interior temperature decreases, which results in stronger cold downwellings, which are less susceptible to slab-detachment.

In the last numerical experiment, we have studied an end-member case, where a higher thermal conductivity $k = 1 + 10(T_0 + T)^3$ is restricted only to a layer below the ppv transition and the rest of the mantle is characterized by a constant conductivity $k = 1$. The results are shown in Fig. 7. An increased thermal conductivity in the bottom boundary layer alone is sufficient to produce large hot upwellings at the bottom of the lower mantle. Above these lower mantle upwellings, there is a hot low viscosity layer just at the 670 km boundary, which was revealed by Kido and Čadek (1997) below the oceanic regions. This result demonstrates the importance of the released latent heat associated with the endothermic phase change, where the material from the superplume heads penetrating the 670 km interface is heated up by both latent heat and viscous dissipation, which produce a local increase in the temperature, this effect was studied in detail by Steinbach and Yuen (1994) in convection models with only an endothermic phase transition at 670 km depth and constant thermal conductivity. This layer then becomes a source of secondary upper mantle plumes, which are able to survive and are not diffused, as the radiative heat transfer in this model is now considered to be negligible everywhere except in the D″ layer. The character of this partially layered convection is probably even better demonstrated by means of the streamlines, where the "two modes" of convection can be clearly recognized: "the first mode" consists of large lower mantle convection cells with a global character, whereas the "second mode" is produced by a local upward penetration of the 670 km boundary, followed then by smaller upper mantle convection cells, which are irregularly distorted in the horizontal direction due to interactions between these two modes of convection.

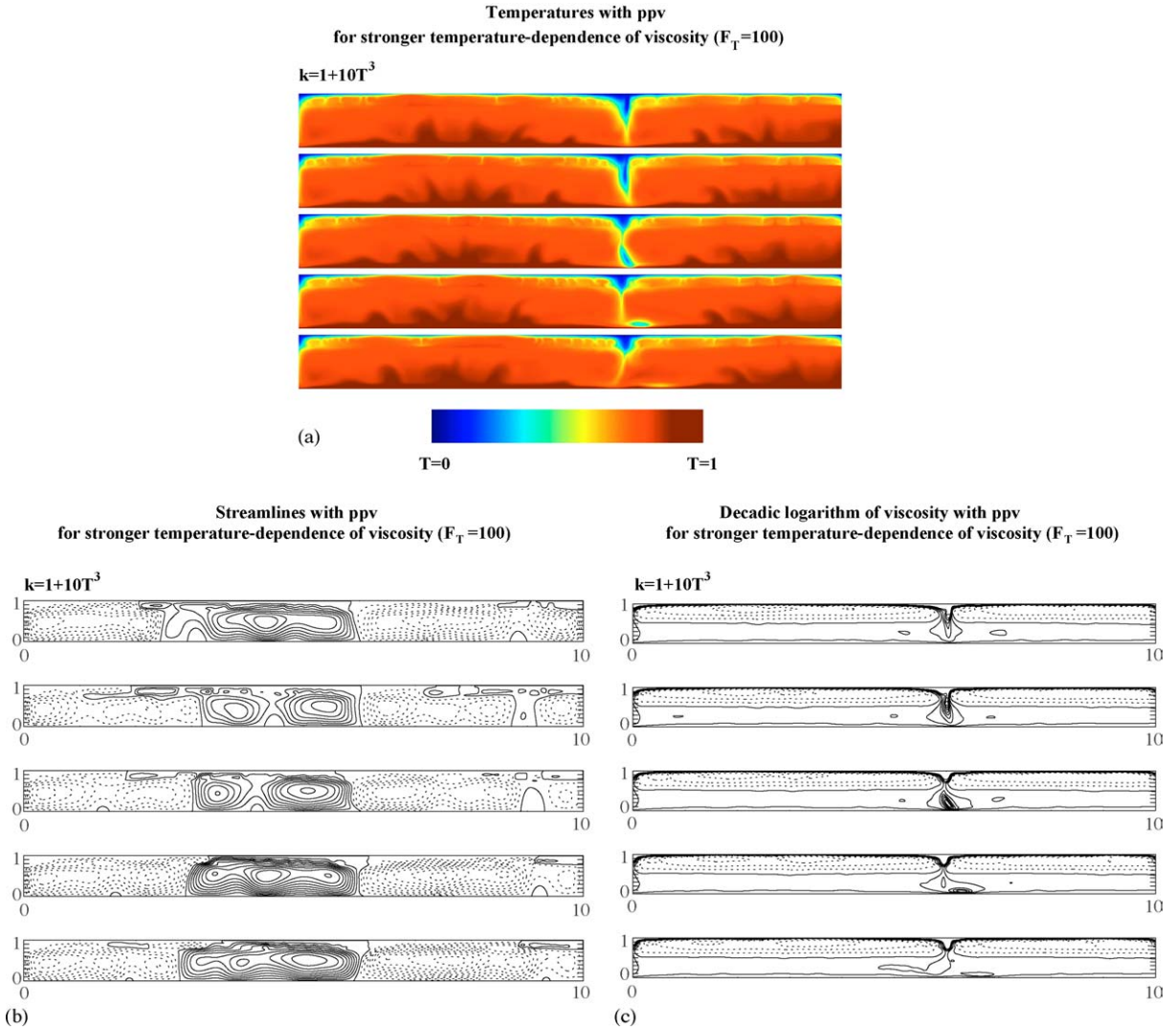

Fig. 5. (a) The same as in Fig. 2 but an exothermic phase transition with $P = 0.10$ was added at 2650 km depth, stronger temperature-dependence of viscosity ($F_T = 100$) was considered and only the case $k = 1 + 10(T_0 + T)^3$ is shown. Dimensionless time-steps between the subsequent panels are 8×10^{-4}. (b) Streamlines of the mantle flow and (c) decadic logarithm of dimensionless viscosity corresponding to the temperature fields at each time-step shown in (a). All fields are constructed in the same way as in Fig. 3.

To further demonstrate details of heat transfer in such a complicated model, we present the local Bullen parameter introduced by Matyska and Yuen (2002) in Fig. 7d. Superadiabatic vertical gradient of temperature is characterized by values lower than 1 and subadiabatic gradient yields values higher than 1. At 670 km boundary, we can clearly recognize both subadiabatic gradients caused by local heating and superadiabatic layer, which is the result of partial layering.

In order to summarize the influence of changes of thermal conductivity and/or viscosity in our models to obtained temperatures, we present typical geotherms (i.e. horizontally averaged temperatures) of the four studied cases in Fig. 8. We can see that an increase of temperature in the lower mantle can be substantial due to incorporating both radiative transfer of heat and temperature-dependence of viscosity. On the other hand, partial layering is typical only for the case, where an increase of thermal conductivity was confined to the D″ layer. The surface Nusselt numbers of our models lie usually between 15 and 30, corresponding to realistic geophysical expectations (e.g. Mc Namara and van Keken, 2000). However, partial layering obtained in the last model can result in the surface Nusselt number slightly lower than 10, although the temperature in the lower mantle is relatively high. The influence of radiative thermal conduc-

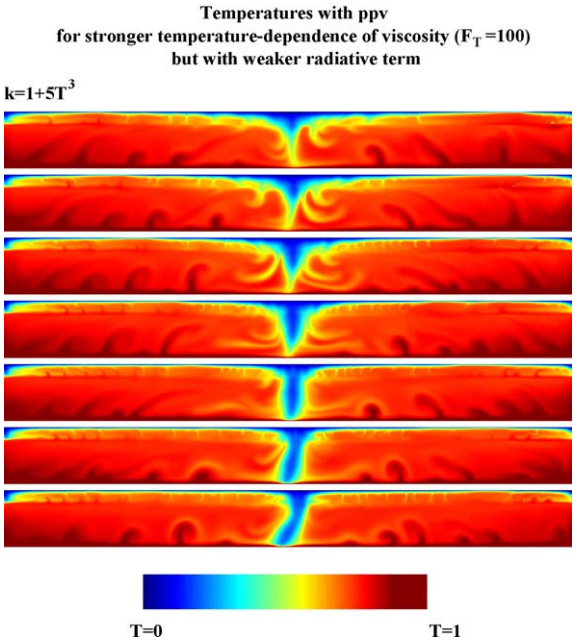

Fig. 6. The same as in Fig. 5a but with a weaker radiative thermal conductivity term $k = 1 + 5(T_0 + T)^3$ was considered. Dimensionless time-steps between the subsequent panels are 2.5×10^{-4}.

tivity is to decrease the temperature gradient in the D″ layer, on which seismic constraints can be placed (e.g. Kuo and Chen, 2005).

4. Discussion and concluding remarks

The recently discovered post-perovskite phase transition (Murakami et al., 2004) has important ramifications on mantle dynamics, because of its potential impact on amplifying the development of bottom boundary layer instabilities. This salient point was driven home by the calculations of both Nakagawa and Tackley (2004) and Matyska and Yuen (2005), who demonstrated that small-scale instabilities would prevail in the D″ layer. In order to obtain any sort of large-scale upwellings, as inferred for example by seismic modelling under Africa (e.g. Ni and Helmberger., 2003), Matyska and Yuen (2005) have found it necessary to invoke some amount of radiative heat transfer in the presence of a depth-dependent lower mantle viscosity. In this work, we have further demonstrated this mechanism for producing large-scale lower mantle upwellings is still effective even with temperature-dependent viscosity, which tends to produce short-wavelength instabilities (Yuen and Peltier, 1980; Olson et al., 1987). An increase of thermal conductivity from the T^3 radiative term thus exerts the most impact in our convection models, as realistic velocities of the order of 5 cm/year, which are similar to those of subducting plates, are attained in the flow, in contrast to lower velocities with constant thermal conductivity. On the other hand, influence of buoyancy and/or latent heat generated by the post-perovskite phase transition is only of minor importance.

As demonstrated by our last model in which the radiative thermal conductivity is only restricted to the post-perovskite phase (see Fig. 7), the flow fields are found to be greatly influenced by the presence of radiative thermal conductivity, which acts in concert with the ppv transition. Much higher buoyancy is produced in the large upwellings, which are endowed with a higher upward-carrying capacity. Upon reaching the perovskite to spinel transition, heat is liberated and a large pool of hot low viscosity material is generated, which facilitates mechanical decoupling between the upper and lower mantle circulations and results in partial layering, see also discussion of this decoupling mechanism in Cserepes and Yuen (1997) and Čížková et al. (1999). On the other hand, with constant thermal conductivity there are many thin upwellings, which are not favorable to the production of a significant low viscosity zone under the 670 km phase change, which was unveiled by Kido and Čadek (1997) and modelled by Cserepes and Yuen (1997) and Čížková et al. (1999). Thus, whole-mantle convection is preferred in the case of constant thermal conductivity with the ppv transition. The other consequence of both higher buoyancy of lower mantle superplumes with a lower viscosity is an increase of the convective velocity. A basal layer with high thermal conductivity is thus sufficient to cause the formation of large-scale upwellings, because of the non-linear heat diffusing effect at the base of the plume. Results from purely layered conductivity models of Yanagawa et al. (2004) also show that large-scale upwellings are promoted by a thin high conductivity layer at the base of the mantle. This notion of a high-conductivity layer has been suggested on geochemical grounds of iron infiltration from the outer core by Manga and Jeanloz (1996). Alternatively, a high conductivity layer may also come from a putative layer of FeS, which also has an unusually high thermal conductivity (Hofmeister and Criss, 2005). Note here that recent work by Kameyama and Yuen (submitted for publication) in 3-D has shown the same kind of physics as for 2-D.

The ultimate consequence of the post-perovskite transition at the base of the mantle, because of its peculiar location close to the CMB, is to drive mantle convection toward a more asymmetric pattern. The favored scenario would have large plumes in the lower mantle and secondary upwellings being launched from the semi-impermeable boundary layer at the 670 km phase

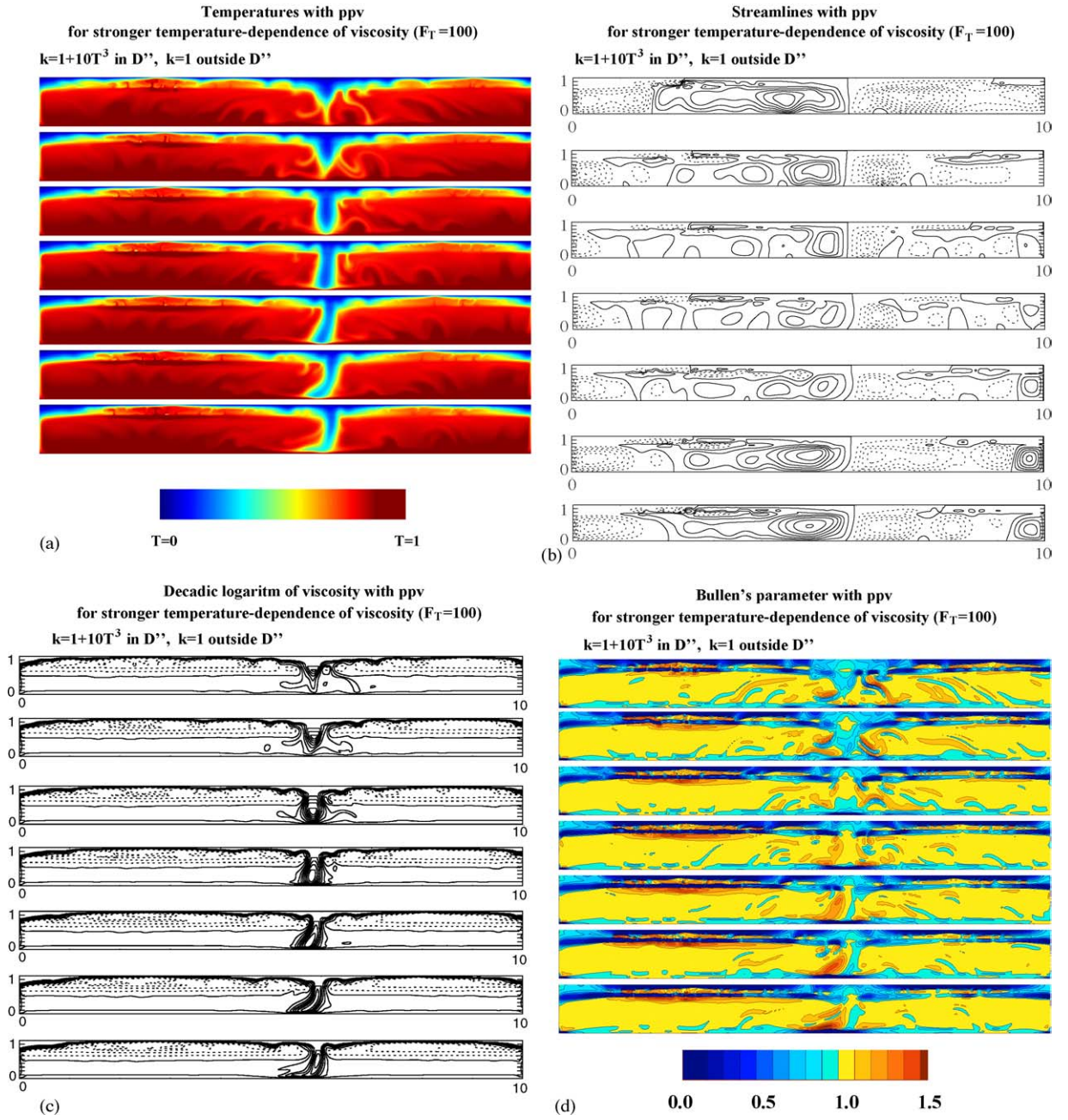

Fig. 7. (a) The same as in Fig. 5a but thermal conductivity with stronger radiative term, i.e. $k = 1 + 10(T_0 + T)^3$, was employed only below the 2650 km depth, only constant conductivity contribution $k = 1$ was considered in the mantle above this interface. Dimensionless time-steps between the subsequent panels are 3×10^{-4}. (b) Streamlines of the mantle flow and (c) decadic logarithm of dimensionless viscosity corresponding to the temperature fields at each time-step shown in (a). These fields are constructed in the same way as in Fig. 3. (d) Local Bullen parameter of the temperature fields displayed in (a).

change, while being supported from below by a low viscosity region (Kido and Čadek, 1997) and perhaps also from the 400 km phase boundary due to Rayleigh–Taylor instabilities induced locally by volatiles (Bercovici and Karato, 2003; Gerya and Yuen, 2003). At the same time many of the slabs would lose their thermal identity (e.g. van der Hilst and Kárason, 1999) by the combined effects of radiative thermal conductivity and latent heat release by the post-perovskite transition. The downward cold flow in the lower mantle would thus be dispersed. Thus

'geoth1': with ppv; $F_T = 10$; $k = 1$ Nu = 19.3
'geoth2': with ppv; $F_T = 10$; $k = 1 + 1.0T^3$ Nu = 30.1
'geoth3': with ppv; $F_T = 100$; $k = 1 + 1.0T^3$ Nu = 20.8
'geoth4': with ppv; $F_T = 100$; $k = 1 + 1.0T^3$ only in D" Nu = 8.2

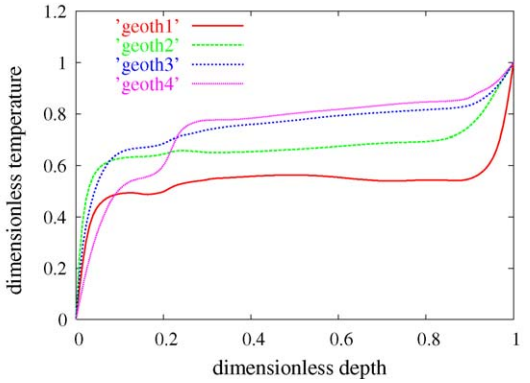

Fig. 8. Typical geotherms (horizontally averaged dimensionless temperatures) of the cases displayed in Figs. 3, 5 and 7. The symbol *Nu* denotes the Nusselt number, i.e. the gradient of the curves at $z = 0$.

a gross asymmetry in the vertical heat and mass transfer, accompanied by partial-layered convection, would develop under these circumstances, which would strongly impact on the thermal history of the mantle. Since the post-perovskite phase might not have formed in a young hot Earth (Oganov and Ono, 2004), this asymmetric pattern might have prevailed only after a certain period in the Earth's thermal history. A strong secular change in the bottom boundary condition for mantle convection is thus a distinct possibility. Enhanced Joule heating (Braginskii and Meitlis, 1987; Matyska and Moser, 1994) due to an increase of electrical conductivity at the base of the mantle from electronic transitions (Badro et al., 2004; Li et al., 2005) in the D″ layer can also influence the thermal–electrical coupling between the core and the lower mantle. Finally, chemical variations on the dynamics of the phase boundary are also significant and cannot be neglected in the future, since there are now some firm experimental evidence that phase boundary distortions can be significant with chemical variations (Mao et al., 2004).

Acknowledgements

The authors would like to thank discussions with Anne Hofmeister, Dick Peltier, Nick Petford, Renata Wentzcovitch, Frank J. Spera, Arie van den Berg, Rob van der Hilst and Marc Monnereau. Constructive comments of Zhang Huai and an anonymous reviewer helped to improve quality of the text. This research has been supported by the Czech Grant Agency grant 205/03/0778 and grants from the CSEDI and ITR programs of the National Science Foundation.

References

Badro, J., Fiquet, G., Guyot, F., Rueff, J.-P., Struzhkin, V.V., Vankó, G., Monaco, G., 2003. Iron partitioning in Earth's mantle: toward a deep lower mantle discontinuity. Science 300, 789–791.

Badro, J., Rueff, J.-P., Vankó, G., Monaco, G., Fiquet, G., Guyot, F., 2004. Electronic transitions in perovskite: Possible non-convecting layers in the lower mantle. Science 305, 383–386.

Bercovici, D., Karato, S.-I., 2003. Whole-mantle convection and the transition-zone water filter. Nature 425, 39–44.

Braginskii, S.I., Meitlis, V.P., 1987. Overheating instability in the lower mantle near the boundary with the core, Izvestiya. Earth Phys. 23, 646–649.

Brown, J.M., 1986. Interpretation of the D″ zone at the base of the mantle: dependence on asumed values of thermal conductivity. Geophys. Res. Lett. 13, 1509–1512.

Christensen, U.R., Yuen, D.A., 1985. Layered convection induced by phase transitions. J. Geophys. Res. 90, 10291–10300.

Čížková, H., Čadek, O., van den Berg, A.P., Vlaar, N.J., 1999. Can lower mantle slab-like seismic anomalies be explained by thermal coupling between the upper and lower mantles? Geophys. Res. Lett. 26, 1501–1504.

Cserepes, L., Yuen, D.A., 1997. Dynamical consequences of mid-mantle viscosity stratification on mantle flows with an endothermic phase transition. Geophys. Res. Lett. 24, 181–184.

Davies, G.F., 1999. Dynamic Earth. Cambridge University Press.

Dubuffet, F., Yuen, D.A., Rainey, E.S.G., 2002. Controlling thermal chaos in the mantle by positive feedback from radiative thermal conductivity. Nonlinear Process. Geophys. 9, 311–323.

Forte, A.M., Mitrovica, J.X., 2001. Deep-mantle high-viscosity flow and thermochemical structure inferred from seismic and geodynamic data. Nature 410, 1049–1056.

Fukao, Y., Obayashi, M., Inoue, H., Nenbai, M., 1992. Subducting slabs stagnant in the mantle transition zone. J. Geophys. Res. 97, 4809–4822.

Garnero, E.J., 2000. Heterogeneity of the lowermost mantle. Annu. Rev. Earth Planet. Sci. 28, 509–537.

Gerya, T.V., Yuen, D.A., 2003. Rayleigh–Taylor instabilities from hydration and melting propel 'cold plumes' at subduction zones. Earth Planet. Sci. Lett. 212, 47–62.

Hansen, U., Yuen, D.A., Kroening, S.E., Larsen, T.B., 1993. Dynamical consequences of depth-dependent thermal expansivity and viscosity on mantle circulations and thermal structure. Phys. Earth Planet. Inter. 77, 205–223.

Hanyk, L., Moser, J., Yuen, D.A., Matyska, C., 1995. Time-domain approach for the transient responses in stratified viscoelastic Earth. Geophys. Res. Lett. 22, 1285–1288.

Hauck, S.A., Phillips, R.J., Hofmeister, A.M., 1999. Variable conductivity: effects on the thermal structure of subducting slabs. Geophys. Res. Lett. 26, 3257–3260.

Hofmeister, A.M., 1999. Mantle values of thermal conductivity and the geotherm from phonon lifetimes. Science 283, 1699–1706.

Hofmeister, A.M., 2005. The dependence of diffusive radiative transfer on grain-size, temperature and Fe-content: implications for mantle processes. J. Geodyn. 40, 51–72.

Hofmeister, A.M., Criss, R.E., 2005. Earth's heat flux revised and linked to chemistry. Tectonophysics 395, 159–177.

Hofmeister, A.M., Yuen, D.A. The threshold dependencies of thermal conductivity and implications on mantle dynamics. Earth Planet. Space, submitted for publication.

Iitaka, T., Hirose, K., Kawamura, K., Murakami, M., 2004. The elasticity of the $MgSiO_3$ post-perovskite phase in the Earth's lowermost mantle. Nature 430, 442–444.

Kameyama, M., Yuen, D.A. Enhanced heating of the deep mantle by post-perovskite phase transition. Earth Planet. Sci. Lett., submitted for publication.

Kido, M., Čadek, O., 1997. Inferences of viscosity from the oceanic geoid: Indication of a low viscosity zone below the 660-km discontinuity. Earth Planet. Sci. Lett. 151, 125–137.

Kuo, B.Y., Chen, C.W., 2005. A seismological determination of the temperature gradient in D′′ beneath the western Pacific. J. Geophys. Res. 110 (B0), 5304.

Lay, T., Garnero, E.J., William, Q., 2004. Partial melting in a thermo-chemical boundary layer at the base of the mantle. Phys. Earth Planet. Inter. 146, 441–467.

Leitch, A.M., Yuen, D.A., 1989. Internal heating and thermal constraints on the mantle. Geophys. Res. Lett. 16, 1407–1410.

Li, L., Brodholt, J., Stackhouse, S., Weidner, D.J., Alfredsson, M., Price, G.D., 2005. Electronic spin state of ferric iron in Al-bearing perovskite in the lower mantle. Geophys. Res. Lett. 32 (17), Art No L17307.

Mc Namara, A.K., van Keken, P.E., 2000. Cooling of the Earth: a parameterized convection study of whole versus layered models. Geochem. Geophys. Geosyst. 1. Paper number 2000GC000045.

Manga, M., Jeanloz, R., 1996. Implications of a metal-bearing chemical boundary layer in D" for mantle dynamics. Geophys. Res. Lett. 23, 3091–3094.

Mao, W.L., Shen, G., Prakapenka, V.B., Meng, Y., Cambell, A.J., Heinz, D.L., Shu, J., Hemley, R.J., Mao, H., 2004. Ferromagnesian postperovskite silicates in the D′′ layer of the Earth. Proc. Natl. Acad. Sci. U.S.A. 101, 15867–15869.

Marton, F.C., Cohen, R.E., 2002. Constraints on lower-mantle composition from molecular dynamics of $MgSiO_3$ perovskite. Phys. Earth Planet. Inter. 134, 239–252.

Maruyama, S., 1994. Plume tectonics. J. Geol. Soc. Jpn. 100, 24–49.

Matyska, C., Moser, J., 1994. Heating in the D′′-layer and the style of mantle convection. Studia Geophys. Geod. 38, 286–292.

Matyska, C., Moser, J., Yuen, D.A., 1994. The potential influence of radiative heat transfer on the formation of megaplumes in the lower mantle. Earth Planet. Sci. Lett. 125, 255–266.

Matyska, C., Yuen, D.A., 2001. Are mantle plumes adiabatic? Earth Planet. Sci. Lett. 189, 165–176.

Matyska, C., Yuen, D.A., 2002. Bullen's parameter η: a link between seismology and geodynamical modelling. Earth Planet. Sci. Lett. 198, 471–483.

Matyska, C., Yuen, D.A., 2000. Profiles of the Bullen parameter from mantle convection modelling. Earth Planet. Sci. Lett. 178, 39–46.

Matyska, C., Yuen, D.A., 2005. The importance of radiative heat transfer on superplumes in the lower mantle with the new post-perovskite phase change. Earth Planet. Sci Lett. 234, 71–81.

Mitrovica, J.X., Forte, A.M., 2004. A new inference of mantle viscosity based upon joint inversion of convection and glacial isostatic adjustment data. Earth Planet. Sci. Lett. 225, 177–189.

Murakami, M., Hirose, K., Kawamura, K., Sata, N., Ohishi, Y., 2004. Post-perovskite phase transition in $MgSiO_3$. Science 304, 855–858.

Nakagawa, T., Tackley, P.J., 2004. Effects of a perovskite-post perovskite phase change near core–mantle boundary in compressible mantle convection. Geophys. Res. Lett. 31, L16611.

Ni, S.D., Helmberger, D.V., 2003. Seismological constraints on the South African superplume; could be the oldest distinct structure on Earth. Earth Planet. Sci. Lett. 206, 119–131.

Oganov, A.R., Ono, S., 2004. Theoretical and experimental evidence for a post-perovskite phase of $MgSiO_3$ in Earth's D′′ layer. Nature 430, 445–448.

Olson, P., Schubert, G., Anderson, C., 1987. Plume formation in the D′′-layer and the rougness of the core–mantle boundary. Nature 327, 409–415.

Ricard, Y., Wuming, B., 1991. Inferring viscosity and the 3-D density structure of the mantle from geoid, topography and plate velocities. Geophys. J. Int. 105, 561–572.

Schubert, G., Masters, G., Olson, P., Tackley, P., 2004. Superplumes or plume clusters? Phys. Earth Planet. Inter. 146, 147–162.

Schuster, H.G., 1984. Deterministic Chaos: An Introduction. Physik Verlag, GmbH, Weinheim, 220 pp.

Steinbach, V., Yuen, D.A., 1994. Melting instabilities in the transition zone. Earth Planet. Sci. Lett. 127, 67–75.

Su, W.-J., Dziewonski, A.M., 1991. Predominance of long-wavelength heterogeneity in the mantle. Nature 352, 121–126.

Takeuchi, N., Kobayashi, M., 2004. Improvement of seismological earth models by using data weighting in waveform inversion. Geophys. J. Int. 158, 681–694.

Tsuchiya, T., Tsuchiya, J., Umemoto, K., Wentzcovitch, R.M., 2004. Phase transition in $MgSiO_3$ perovskite in the earth's lower mantle. Earth Planet. Sci. Lett. 224, 241–248.

Turcotte, D.L., Schubert, G., 2002. Geodynamics, second ed. Cambridge University Press.

van den Berg, A.P., Yuen, D.A., 1998. Modelling planetary dynamics by using the temperature at the core–mantle boundary as a control variable: effects of rheological layering on mantle heat transport. Phys. Earth Planet. Inter. 108, 219–234.

van den Berg, A.P., Yuen, D.A., Allwardt, J.R., 2002. Non-linear effects from variable thermal conductivity and mantle internal heating: implications for massive melting and secular cooling of the mantle. Phys. Earth Planet. Inter. 129, 359–375.

van der Hilst, R., Engdahl, R., Spakman, W., Nolet, G., 1991. Tomographic imaging of subducted lithosphere below northwest Pacific island arcs. Nature 353, 37–43.

van der Hilst, R.D., Kárason, H., 1999. Compositional heterogeneity in the bottom 1000 kilometers of Earth's mantle: Toward a hybrid convection model. Science 283, 1885–1888.

Vincent, A.P., Yuen, D.A., 1988. Thermal attractor in chaotic convection with high Prandtl number fluids. Phys. Rev. A 38, 328–334.

Yanagawa, T.K.B., Nakada, M., Yuen, D.A., 2004. A simplified mantle convection model for thermal conductivity stratification. Phys. Earth Planet. Inter. 146, 163–177.

Yuen, D.A., Peltier, W.R., 1980. Mantle plumes and the thermal stability of the D′′ layer. Geophys. Res. Lett. 7, 625–628.

Zhao, W., Yuen, D.A., 1987. The effects of adiabatic and viscous heatings on plumes. Geophys. Res. Lett. 14, 1223–1227.

Zhao, D., 2001. Seismic structure and origin of hotspots and mantle plumes. Earth Planet. Sci. Lett. 192, 251–265.

Zhao, D., 2004. Global tomographic images of mantle plumes and subducting slabs: insight into deep Earth dynamics. Phys. Earth Planet. Inter. 146, 3–34.